CHEMICAL ENGINEERING TRANSACTIONS
VOL. 65, 2018
A publication of AIDIC
The Italian Association of Chemical Engineering
Online at www.aidic.it/cet
Guest Editors: Eliseo Ranzi, Mario Costa

ISBN 978-88-95608- 62-4; **ISSN** 2283-9216

Detailed Kinetics of Pyrolysis and Combustion of Catechol and Guaiacol, as Reference Components of Bio-Oil from Biomass

Carlo Cavallotti, Alberto Cuoci, Tiziano Faravelli, Alessio Frassoldati, Matteo Pelucchi, Eliseo Ranzi

Department of Chemistry, Materials, and Chemical Engineering. Politecnico di Milano. Italy
matteo.pelucchi@polimi.it

Fast biomass pyrolysis is an effective process to produce bio-oils thus allowing to partially replace non-renewable fossil fuels. Bio-oils are complex mixtures with a great amount of large oxygenated organic species, such as substituted phenolic components. Although experimental and kinetic modeling studies of phenol and anisole pyrolysis and combustion are available in the literature, only a minor attention has been devoted to kinetic mechanisms of substituted phenolic species, such as catechol and guaiacol. Multiple substitutions on aromatic ring can originate proximity effects and thus significantly modify bond energies, consequently affecting reaction pathways. Careful evaluations of bond dissociation energies and reference kinetic parameters, based on theoretical computations, are first performed. Guaiacol and catechol pyrolysis and combustion reactions are then compared with the corresponding phenol and anisole mechanisms. This kinetic study allows to identify some preliminary rate rules useful to validate a detailed kinetic mechanism of bio-oil pyrolysis and combustion.

1. Introduction

Biomass fast pyrolysis is typically conducted at moderate temperatures (700-800 K) and short residence times, thus allowing the production of a bio-oil, obtained from the condensation of tars and gases released in the process (Oasmaa et al., 2009). Bio-oils are mostly constituted by large oxygenated species, including substituted phenols (~30% wt, Bertero et al., 2012). Because of the complexity of this liquid mixture, it is clearly unrealistic to develop detailed kinetic models for all the bio-oil components. Thus, reference fuels and their surrogate mixtures are commonly used to predict and reproduce main combustion characteristics of bio-oils. In an attempt to better characterize the combustion of bio-oils, this work extends the CRECK kinetic mechanism of phenol and anisole to include also phenolic species carrying multiple substitutions (Saggese et al., 2013). As widely known, proximity effects of different substituents can change bond energies in doubly substituted benzenes, strongly impacting reaction pathways of pyrolysis and oxidation. Suryan et al. (1988) already observed the large decrease in the dissociation energy of O-CH_3 bond in guaiacol compared to anisole, because of the effect of -OH in ortho position. Similar effects, systematically studied by Ince et al. (2017), are reasonably expected by multiple substitutions on the aromatic ring. In particular, this work focuses on the kinetics of catechol (1,2-dihydroxybenzene) and guaiacol (2-methoxyphenol) pyrolysis and oxidation, providing a preliminary characterization of reaction pathways characteristic of substituted phenolic species together with rate rules, which will allow for further extensions to more complex oxygenated species, such as vanillin (4-hydroxy-3-methoxybenzaldehyde).

2. Assessment of Bond Dissociation Energies (BDE)

2.1 Calculation methods

Insertion of different functional groups on an aromatic ring strongly impacts bond dissociation energies of vicinal bonds (Ince et al., 2017). To systematically investigate such effects, bond dissociation energies have been calculated for a series of compounds, as reported in Figure 1. Starting from phenol, catechol BDEs have been investigated to highlight possible effects of the insertion of an additional hydroxyl group in ortho position. Similarly, salicylaldehyde (2-hydroxybenzaldehyde) can be obtained from benzaldehyde, and guaiacol from anisole (metoxybenzene). The assessment of BDEs presented in the followings provides the basis for the definition of rate rules to describe guaiacol and catechol oxidation and pyrolysis

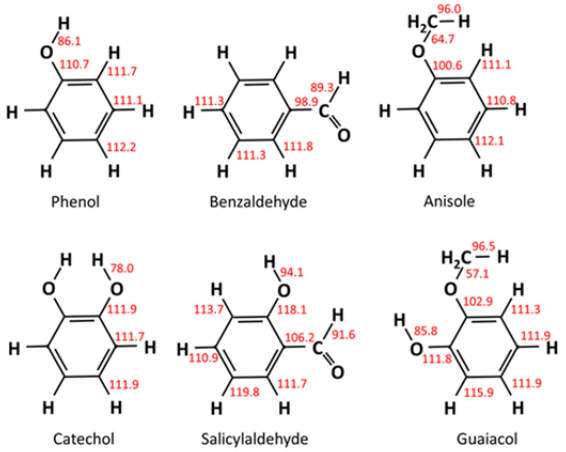

Figure 1: BDEs of aromatics and substituted phenolic compounds at 298 K (kcal/mol).

The outstanding study of Ince et al. (2017) recently provided thermodynamic properties of ~150 substituted aromatic species together with their radicals (~370), generating a database of key thermochemical properties using the G4 method, with bond additivity corrections (BAC). The G4 method implements a specific calculation method. Starting from geometry optimization and frequencies computation at the B3LYP/6-31G(2df,p) level, single point energies are obtained through a first HF limit calculation, followed by a series of MP4 calculations with increasing size basis sets (6-31G(d), 6-31+G(d), 6-31G(2df,p), 6-31G(d)) and finally through a coupled cluster with perturbative inclusions of triples (CCSD(T)). The G4 method typically provides thermochemical properties with a 2σ uncertainty of ~1.1 kcal/mol, which clearly improves the 2σ uncertainty of ~2.5 kcal/mol of the CBS-QB3 method (Klippenstein, 2017). The method we decided to adopt herein aims at approaching a similar accuracy. To optimize geometries and to map rovibrational properties, the M06-2X method is adopted with a 6-311+G(d,p) basis set, which provides higher quality geometries than in the G4 method since the M06-2X functional is able to account for non bonding interactions, differently from the B3LYP functional. Minimum energy structures are determined stochastically sampling the dihedral angles of internal rotations to generate uncorrelated guess geometries, which are successively optimized.
Single point energies are obtained from CCSD(T)/aug-cc-pVTZ energies, corrected for basis set size with the difference betweenf DF-MP2/aug-cc-pVQZ and DF-MP2/aug-cc-pVTZ energies. It should be noted that the coupled cluster calculations are performed using a basis set that is significantly larger than adopted in the G4 protocol. Single point energies are finally calculated as:

$$E = E_{CCSD(T)/aug\text{-}cc\text{-}pVTZ} + E_{DF\text{-}MP2/aug\text{-}cc\text{-}pVQZ} - E_{DF\text{-}MP2/aug\text{-}cc\text{-}pVTZ}\,. \quad (1)$$

2.2 Obtained results and proximity effects

Results from our calculations are reported in Figure 1, and compared in Figure 2 with the values of Ince et al. (2017). The two calculations generally agree within ~0.5-1.5 kcal/mol, as expected from the accuracy of the two methods briefly discussed above. The O-H bond in phenol is the weakest, with a dissociation energy of ~86.1 kcal/mol, followed by that of C-O (~110.7) which is comparable to the remaining aromatic C-H bonds (111.1-112.2 kcal/mol). The BDE of 89.3 kcal/mol of the C-H bond at the carbonyl moiety is the lowest in benzaldehyde. The fission of the O-C bond, connecting the carbonyl function to the aromatic ring, requires 98.9 kcal/mol. Again, C-H bonds on the aromatic ring maintain the previous values of 111.5-112.2 kcal/mol. Anisole initiation most likely occurs breaking the O-C bond in the methoxy group forming methyl and phenoxy

radical, requiring only 64.7 kcal/mol. The primary C-H bond in methyl group has a BDE of 96.0 kcal/mol, whereas the BDE of C-OCH_3 bond is 100.6 kcal/mol. Figure 2 summarizes the effect on the BDEs of an additional substitution of OH, in ortho position. ΔBDEs with respect to the characterizing functional group of the starting molecules (-OH in phenol, -(C=O)H in benzaldehyde and –OCH_3 in anisole). This figure also shows the very satisfactory agreement with the deviations reported by (Ince et al., 2017).

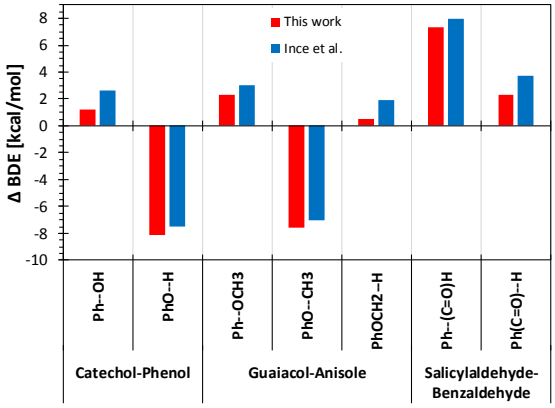

Figure 2. Effect on BDEs of an additional OH substitution in ortho position. ΔBDEs are the differences of BDE between bi- and corresponding mono- substituted species.

Concerning phenol and catechol, the additional OH substitution weakens the O-H bond of 7.5-8.1 kcal/mol, whereas the C-O bond becomes 1-2.5 kcal/mol stronger. Similarly, the O-CH_3 bond is weakened by ~7-7.6 kcal/mol in guaiacol, because of the additional OH substitution. Compared to anisole, guaiacol C-OCH_3 bond is 2.3-3 kcal/mol stronger, and the primary C-H bond in the methyl group is increased by 0.5-1.9 kcal/mol.
When comparing salicylaldehyde and benzaldehyde, an increase in BDEs is observed for both the C-C bond connecting the carbonyl group to the aromatic ring (7-8 kcal/mol), and the weaker C-H bond in the carbonyl moiety (2-3 kcal/mol). Because of the additional OH group, there is a systematic increase of the BDE of C-H bonds forming phenyl like radicals for all phenolic species. In the case of salicylaldehyde, the BDE of the C-H bond in ortho position to the hydroxyl moiety increases by ∼2 kcal/mol. A similar variation for the analogous position is observed for guaiacol, with BDE in the order of 116 kcal/mol. Moreover, a larger increase of ∼7 kcal/mol is observed in salicylaldehyde for the C-H bond in para-position with respect to the OH group.

3. Kinetic mechanism and model validation

Pelucchi et al. (2018) already discussed and presented relevant reactions of phenol, and anisole with several comparisons with experimental data. Anisole pyrolysis shows a significant formation of cresols, guaiacol, and benzaldehyde, together with benzo- and and dibenzofuran (Nowakowska et al. 2014). Vasiliou et al. (2013) studied the high temperature thermal decomposition mechanisms of furfural and benzaldehyde in a micro-tubular flow reactor, whereas Grela and Colussi (1986) explored benzaldehyde pyrolysis. Here, a greater attention is devoted to kinetic mechanisms of catechol and guaiacol.

3.1 Catechol

Ledesma and coworkers thoughtfully analyzed specific reactions of catechol (Ledesma et al., 2002; Wornat et al., 2001; Tomas et al., 2007). Altarawneh et al. (2010) theoretically studied the unimolecular decomposition channels of catechol, and they found that at temperatures lower than 1000 K, the hydroxyl H migration to a neighboring ortho carbon bearing an H atom is a dominant channel with CO and butadiene formation (Figure 3)

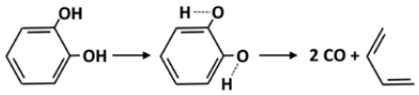

Figure 3. Molecular reaction of catechol, producing butadiene and CO.

At higher temperatures, a concerted, intra-molecular water elimination process (Figure 4) from the two hydroxyl group results in the formation of cyclopenta-2,4-dien-1-ylidenemethanone (C_6H_4O) or epoxy benzene, which then decomposes to form phenoxyl diradicals. These radicals can easily abstract H atoms

during catechol decomposition and form phenoxy radicals or can recombine forming dibenzo-p-dioxin (Lomnicki, et al., 2008)

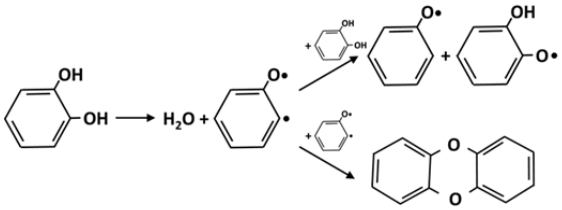

Figure 4. Intramolecular water elimination and successive fate of phenoxy radicals.

Moving from these studies, catechol kinetic mechanism has been developed by using similarity and analogies with phenol kinetics, but also accounting for the significant differences in BDEs. H-abstraction reactions on catechol (Figure 5) form the 2-hydroxy-phenoxyl radical, whose successive decomposition, through the intermediate cyclic C_5H_5O• radical, mainly forms C_2-C_4 acetylenic species (Ledesma et al., 2002):

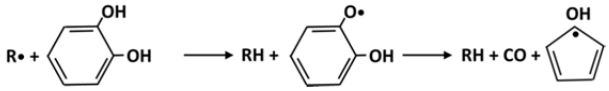

Figure 5. H-abstraction reactions on catechol and decomposition pathway of 2-hydroxy-phenoxyl radical.

Ipso addition reactions (Figure 6) form phenol and cresol:

Figure 6. Ipso-addition reactions on catechol, forming phenol and cresol.

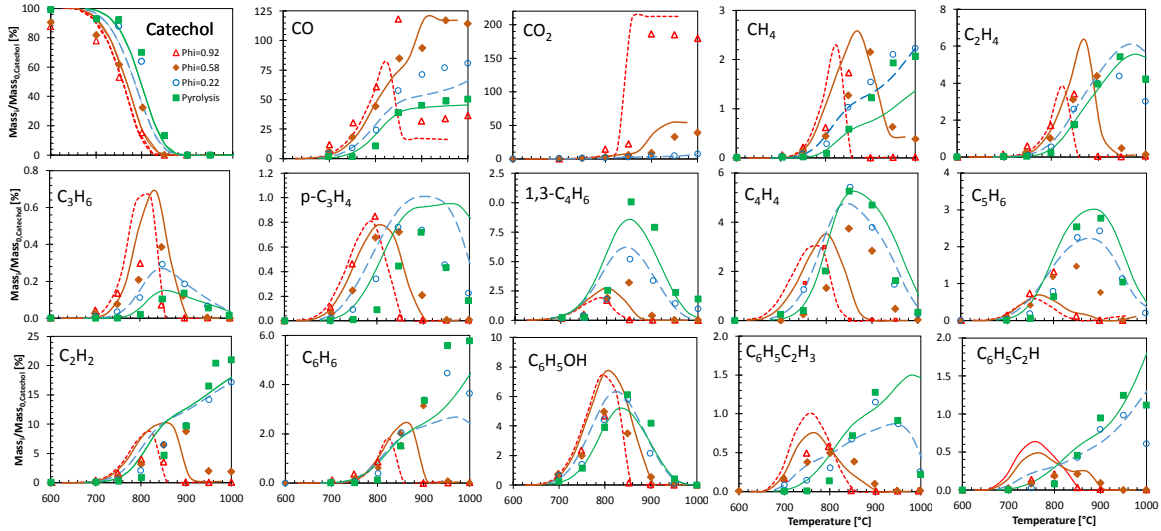

Figure 9. Catechol pyrolysis and oxidation at residence time of 0.3 s and different equivalent ratios. Comparison between model predictions (lines) and experimental data (Thomas et al., 2007). Catechol conversion and mole yields vs temperature [°C].

Figure 9 shows a detailed comparison of model predictions with the experimental data of gas-phase catechol pyrolysis and oxidation with oxygen ratios ranging from 0 (pure pyrolysis) to 0.92 (near stoichiometric oxidation) (Thomas et al., 2007). Experiments were conducted at a residence time of 0.3 s, over a temperature range of 500–1000 °C. Catechol pyrolysis and fuel-rich oxidation produce a range of light hydrocarbons as well as several aromatic hydrocarbons. To understand better the formation of polycyclic

aromatic hydrocarbons (PAH), Thomas and Wornat (2009) performed isothermal pyrolysis experiments with mixtures of catechol with C_2H_2 and C_4H_6.

3.2 Guaiacol

With reference to Figure 1, it is clear that the favored chain initiation reaction of 2-methoxyphenol is the cleavage of the weak phenoxyl–methyl bond with the formation of 2-hydroxyphenoxyl radical, which forms easily catechol via successive H abstraction reactions. As a consequence of internal H-abstraction reactions, the two primary radicals of guaiacol can isomerize and form salicyl-aldehyde with a successive dehydrogenation step, as described in Figure 7 (Kim et al., 2014; Wang et al., JAAP 2016):

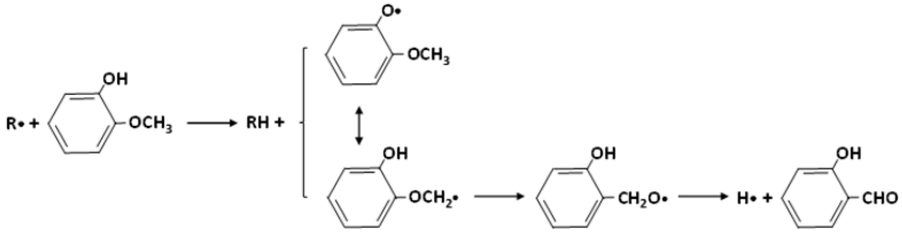

Figure 7. H-abstraction reactions and successive radical isomerization/decomposition pathways.

Again, ipso addition reactions (Figure 8) can form phenol, anisole, cresol, and 2-methyl-anisole:

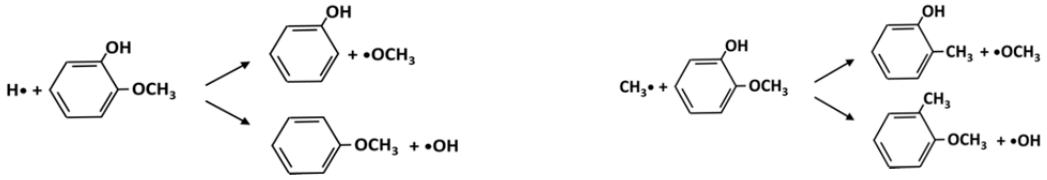

Figure 8. Ipso-addition reactions on guaiacol, forming phenol, anisole, cresol and 2-methyl anisole.

Although catechol, salicyl-aldehyde, and cresol are primary products from guaiacol, phenol is mostly formed by successive reactions of intermediate species, as clearly shown by its experimental and predicted trend with guaiacol conversion in Figure 10. Figure 11 shows further comparisons with experimental data reported by (Lawson and Klein, 1985).

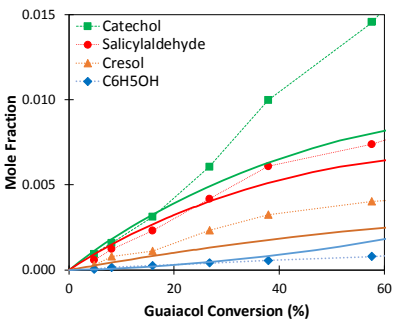

Figure 10. Major products from Guaiacol pyrolysis at 467 °C and 9.5 s. (Dorrestijn and Mulder, 1999)

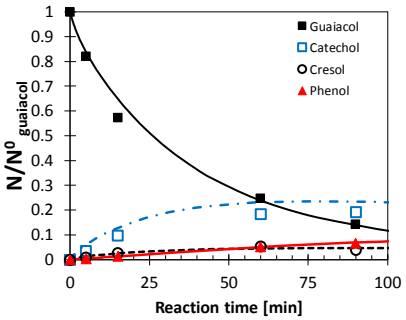

Figure 11. Yields of major products in guaiacol pyrolysis at 383 °C (Lawson and Klein, 1985)

4. Major reaction classes and reaction rules

This kinetic modeling activity already highlights a few general reaction rules for aromatic substituted species. As a matter of facts, the BDEs reported in Figure 1 clearly indicate not only the favored chain initiation reactions, but also support the definition of their high pressure limit rate constants. Similarly, it is possible to derive the selectivity of different H-abstraction reactions and their rate parameters. Further work is mainly required for relevant molecular reactions.

5. Conclusion

This kinetic study further highlights and emphasizes the hierarchical structure of detailed kinetic mechanisms. Whereas the kinetic mechanisms of anisole, guaiacol (2-metoxy-phenol), and catechol (2-hydroxy-phenol) are mainly derived from the gas–phase reactions of phenol and aromatic components, they will constitute the basis for the successive extension of the kinetic mechanism towards the pyrolysis and oxidation of more representative and substituted aromatic compounds such as vanillin (4-hydroxy-3-methoxy-benzaldehyde: C8H8O3) whose intermediate decomposition products are guaiacol, salicylaldehyde, anisole, catechol, and phenol.

Acknowledgments

The authors gratefully acknowledge the partial financial support for this research provided by the European Union under the Horizon 2020 research and innovation programme (Residue2Heat project, G.A. No 654650).

Reference

Altarawneh, M., Dlugogorski, B.Z., Kennedy, E.M. and Mackie, J.C., 2009. Theoretical study of unimolecular decomposition of catechol. The Journal of Physical Chemistry A, 114(2), pp.1060-1067.

Bertero, M., de la Puente, G., & Sedran, U., 2012. Fuels from bio-oils: Bio-oil production from different residual sources, characterization and thermal conditioning. Fuel, 95, pp.263-271.

Dorrestijn, E. and Mulder, P., 1999. The radical-induced decomposition of 2-methoxyphenol. Journal of the Chemical Society, Perkin Transactions 2, (4), pp.777-780.

Grela, M.A. and Colussi, A.J., 1986. Kinetics and mechanism of the thermal decomposition of unsaturated aldehydes: Benzaldehyde, 2-butenal, and 2-furaldehyde. The Journal of Physical Chemistry, 90(3), pp.434-437.

Kim, K.H., Bai, X. and Brown, R.C., 2014. Pyrolysis mechanisms of methoxy substituted α-O-4 lignin dimeric model compounds and detection of free radicals using electron paramagnetic resonance analysis. Journal of Analytical and Applied Pyrolysis, 110, pp.254-263.

Klippenstein, S. J. (2017). From theoretical reaction dynamics to chemical modeling of combustion. Proceedings of the Combustion Institute, 36(1), 77-111.

Ince, A., Carstensen, H.H., Sabbe, M., Reyniers, M.F. and Marin, G.B., 2017. Group additive modeling of substituent effects in monocyclic aromatic hydrocarbon radicals. AIChE J, 63(6), pp.2089-2106.

Lawson, J. R., & Klein, M. T. (1985). Influence of water on guaiacol pyrolysis. Industrial & engineering chemistry fundamentals, 24(2), 203-208.

Ledesma, E.B., Marsh, N.D., Sandrowitz, A.K. and Wornat, M.J., 2002. An experimental study on the thermal decomposition of catechol. Proceedings of the Combustion Institute, 29(2), pp.2299-2306.

Lomnicki, S., Truong, H., & Dellinger, B. (2008). Mechanisms of product formation from the pyrolytic thermal degradation of catechol. Chemosphere, 73(4), 629-633.

Nowakowska, M., Herbinet, O., Dufour, A., & Glaude, P. A. (2014). Detailed kinetic study of anisole pyrolysis and oxidation to understand tar formation during biomass combustion and gasification. Combustion and Flame, 161(6), 1474-1488.

Oasmaa, A., Solantausta, Y., Arpiainen, V., Kuoppala, E., & Sipilä, K. (2009). Fast pyrolysis bio-oils from wood and agricultural residues. Energy & Fuels, 24(2), 1380-1388.

Pelucchi, M., Faravelli, T., Frassoldati, A., Ranzi, E., SriBala, G., Marin, G.B., Van Geem, K.M. (2018). Experimental and kinetic modeling study of pyrolysis and combustion of anisole. Chemical Engineering Transactions, IconBM, Accepted.

Suryan, M. M., Kafafi, S. A., & Stein, S. E. (1989). The thermal decomposition of hydroxy-and methoxy-substituted anisoles. Journal of the American Chemical Society, 111(4), 1423-1429.

Thomas, S., Ledesma, E.B. and Wornat, M.J., 2007. The effects of oxygen on the yields of the thermal decomposition products of catechol under pyrolysis and fuel-rich conditions. Fuel, 86(16), pp.2581-2595.

Thomas, S. and Wornat, M.J., 2009. Polycyclic aromatic hydrocarbons from the co-pyrolysis of catechol and 1, 3-butadiene. Proceedings of the Combustion Institute, 32(1), pp.615-622.

Vasiliou, A.K., Kim, J.H., Ormond, T.K., Piech, K.M., Urness, K.N., Scheer, A.M., Robichaud, D.J., Mukarakate, C., Nimlos, M.R., Daily, J.W. and Guan, Q., 2013. Biomass pyrolysis: thermal decomposition mechanisms of furfural and benzaldehyde. The Journal of chemical physics, 139(10), p.104310.

Wang, M., & Liu, C. (2016). Theoretic studies on decomposition mechanism of o-methoxy phenethyl phenyl ether: Primary and secondary reactions. Journal of Analytical&Applied Pyrolysis, 117, 325-333.

Wornat, M. J., Ledesma, E. B., & Marsh, N. D. (2001). PAH from the pyrolysis of catechol, a model fuel representative of entities in tobacco, coal, and lignin. Fuel, 80(12), 1711-1726.